Tellus (1997), 49A: 528–543
Printed in UK – all rights reserved

TELLUS
ISSN 0280-6495

Weakly non-linear response of a stably stratified shear flow to thermal forcing

By HYE-YEONG CHUN, *Department of Astronomy and Atmospheric Sciences and Global Environment Laboratory, Yonsei University, Seoul 120-749, Korea*

(Manuscript received 24 July 1996; in final form 16 June 1997)

ABSTRACT

Weakly non-linear response of a stably-stratified shear flow without a critical level of specified heating is investigated analytically using the perturbation method. The heating is prescribed to be bell-shaped in the horizontal and uniform from the surface to the non-dimensional heating depth of one, in the vertical. The non-dimensional vertical wind shear varies from 0.1 to 0.6. As the vertical wind shear increases, the magnitude of the zeroth-order (linear) perturbation vertical velocity above the forcing region increases by extracting energy from the mean shear flow. On the other hand, the magnitude of the perturbation horizontal velocity in the forcing region decreases with increasing wind shear because part of the heating is used to compensate for the positive vorticity induced by the positive wind shear. The forcing to the 1st-order equation exists not only in the specified heating region but also above the heating region because of the wind shear. The magnitude of the 1st-order (weakly non-linear) perturbation vertical velocity above the specified forcing region, varies irregularly with vertical wind shear, because the forcing to the 1st-order equation depends non-linearly on the wind shear. In the forcing region, the magnitude of the perturbation horizontal velocity decreases with increasing wind shear due to both the reduced effective forcing results from the compensation of the vorticity by the wind shear and the forcing to the 1st-order equation which decreases with increasing wind shear. The magnitudes of the momentum flux for the zeroth-order and 1st-order perturbations decrease monotonously with increasing wind shear, and the vertical convergence of the momentum flux exists below the forcing top. Above the forcing region, the vertical convergence/divergence of the momentum flux exists for the 1st-order perturbation. It is suggested that vertical convergence/divergence of the momentum flux can influence large-scale mean motion in terms of gravity wave drag; hence, gravity wave drag induced by the thermal forcing should be included in large-scale models.

1. Introduction

Linear response of a stably stratified atmosphere to thermal forcing has been studied analytically with a wide range of applications to mesoscale phenomena such as heat island, orographic-convective precipitation, rain-induced cold pool in convective system, etc. (Smith and Lin, 1982; Lin and Smith, 1986; Raymond, 1986; Lin, 1987; Lin and Chun, 1991; Baik, 1992). Even though these linear studies have contributed much to understanding the basic dynamics of thermally-induced mesoscale circulations, there is an obvious limitation to a real situation where non-linearity becomes important. Recently, Chun and Baik (1994) (CB hereafter) investigated the weakly non-linear response of a stably stratified atmosphere to heating in a uniform flow. They showed that the major non-linearity effect is to produce a strong convergence near the forcing center, regardless of the specified forcing type. This convergence is responsible for producing upward motion at the center of the forcing region that extends upstream.

Vertical shear of the basic-state wind is one of the important factors in mesoscale convective systems. Specifically, vertical wind shear plays a crucial dynamical rôle in the maintenance and generation of long-lived convective systems, by (i) preventing outflow from moving away from the convective system (Thorpe et al., 1980), (ii) balancing the cold-pool induced circulation effecting to spread downshear (Rotunno et al., 1988), (iii) increasing density current speed in multicell storms (Fovell and Ogura, 1989), (iv) controlling characteristics of the cloud forming along an outflow collision line (Droegemeier and Wilhelmson, 1985).

Linear response of a stably stratified atmosphere to thermal forcing in a constant shear flow with (Lin, 1987; Lin and Chun, 1991) and without (Baik, 1992) a critical level was studied analytically. These studies indicated that the flow response is characterized by the Richardson number of the basic flow and the heating/cooling depth. Lin (1987) showed that when a critical level is located in the thermal forcing region, the vertical velocity there is in phase with the thermal forcing for a wide range of the Richardson number. Lin and Chun (1991) showed that the speed of the density current propagating upstream is slowed down by the vertical wind shear in the lower layer because part of the cooling is used to compensate for the positive vorticity produced by the vertical wind shear; accordingly, the effective cooling producing density current become small.

Mesoscale convective phenomena generally reveal non-linear behavior with vertical wind shear that is not accessible to linear analytic study. Thus, an impetus to the study of non-linear response of an atmosphere to thermal forcing stems from a need for a better understanding of mesoscale phenomena. However, as mentioned in CB, in a fully non-linear analytic approach with thermal forcing, there are mathematical difficulties, but a weakly non-linear approach is feasible. In the present study, the weakly non-linear response of a stably stratified atmosphere of heating in a constant shear flow without a critical level, is investigated analytically. In Section 2, governing equations and solutions for the lowest two powers are presented. The energy and momentum flux equations are derived and discussed in Section 3. In Section 4, the effects of vertical wind shear on the weakly non-linear response of a stably stratified atmosphere to heating are discussed. Finally, a summary and conclusions are given in Section 5.

2. Governing equations and solutions

2.1. Governing equations

The governing equations of a 2-dimensional (x–z plane), steady-state, hydrostatic, non-rotating, inviscid, Boussinesq flow in a constant shear flow with thermal forcing can be written as (CB):

$$U\frac{\partial^3\phi}{\partial x\,\partial z^2}+\frac{\partial b}{\partial x}-J\left(\phi,\frac{\partial^2\phi}{\partial z^2}\right)=0, \tag{1}$$

$$U\frac{\partial b}{\partial x}-N^2\frac{\partial\phi}{\partial x}-J(\phi,b)=\frac{g}{c_p T_0}q. \tag{2}$$

Here, ϕ is the perturbation streamfunction defined by $u=\partial\phi/\partial z$ and $w=-\partial\phi/\partial x$, b the perturbation buoyancy, U the basic-state wind, N the Brunt–Vaisala frequency of the basic flow, g the gravitational acceleration, c_p the specific heat at constant pressure, T_0 the basic-state temperature, and q the thermal forcing. The symbol J is the Jacobian defined by $J(A,B)=(\partial A/\partial x)(\partial B/\partial z)-(\partial A/\partial z)(\partial B/\partial x)$. Following CB, (1) and (2) are non-dimensionalized using the following scale parameters.

$$x=L\hat{x},\qquad z=\left(\frac{U_c}{N}\right)\hat{z},$$

$$d=\left(\frac{U_c}{N}\right)\hat{d},\qquad \phi=\left(\frac{gq_cL}{c_pT_0N^2}\right)\hat{\phi},$$

$$b=\left(\frac{gq_cL}{c_pT_0U_c}\right),\qquad q=q_c\hat{q},\qquad U=U_c\hat{U}. \tag{3}$$

Here, variables with carets denote non-dimensional quantities. Note that in CB, $\hat{U}$ is 1 because the basic-state wind is constant. In the present study, the non-dimensional basic-state wind $\hat{U}$ is a function of $\hat{z}$. Substituting (3) into (1) and (2) yields (with all the carets dropped hereafter):

$$U\frac{\partial^3\phi}{\partial x\,\partial z^2}+\frac{\partial b}{\partial x}-\mu J\left(\phi,\frac{\partial^2\phi}{\partial z^2}\right)=0, \tag{4}$$

$$U\frac{\partial b}{\partial x}-\frac{\partial\phi}{\partial x}-\mu J(\phi,b)=q, \tag{5}$$

where

$$\mu=\frac{gq_cL}{c_pT_0NU_c^2}. \tag{6}$$

The parameter μ is called the non-linearity factor of the thermally-induced finite-amplitude waves. The perturbation streamfunction and buoyancy are expanded in small values of the parameter μ.

$$\phi = \phi_0 + \mu\phi_1 + \mu^2\phi_2 + \cdots, \tag{7}$$

$$b = b_0 + \mu b_1 + \mu^2 b_2 + \cdots. \tag{8}$$

Now, assume that the thermal forcing q has only zeroth-order term. In addition, the basic-state wind U is assumed to have only zeroth-order term. Then, the equations of the lowest 2 powers are given by

$$U_0 \frac{\partial^3 \phi_0}{\partial x\, \partial z^2} + \frac{\partial b_0}{\partial x} = 0, \tag{9}$$

$$U_0 \frac{\partial b_0}{\partial x} - \frac{\partial \phi_0}{\partial x} = q_0, \tag{10}$$

$$U_0 \frac{\partial^3 \phi_1}{\partial x\, \partial z^2} + \frac{\partial b_1}{\partial x} = J\left(\phi_0, \frac{\partial^2 \phi_0}{\partial z^2}\right), \tag{11}$$

$$U_0 \frac{\partial b_1}{\partial x} - \frac{\partial \phi_1}{\partial x} = J(\phi_0, b_0). \tag{12}$$

The zeroth-order eqs. (9) and (10) can be reduced to a single equation for the perturbation vertical velocity of:

$$U_0^2 \frac{\partial^2 w_0}{\partial z^2} + w_0 = q_0. \tag{13}$$

Similarly, the first-order equations (11) and (12) can be reduced to

$$U_0^2 \frac{\partial^2 w_1}{\partial z^2} + w_1 = F(x, z), \tag{14}$$

where

$$F(x, z) = -U_0 J\left(\phi_0, \frac{\partial^2 \phi_0}{\partial z^2}\right) + J(\phi_0, b_0). \tag{15}$$

Using (9) and (10), (15) becomes

$$F(x, z) = 2J(\phi_0, b_0) + \frac{\partial U_0}{\partial z} \frac{\partial \phi_0}{\partial x} \frac{\partial^2 \phi_0}{\partial z^2}. \tag{16}$$

The 2nd term in the right-hand side of (16) is related to the basic-state wind shear. In the uniform wind case, the second term is zero. Therefore, (16) is a general expression of $F(x, z)$. We define a one-sided complex Fourier transform pair by:

$$\tilde{G}(k, z) = \frac{1}{\pi} \int_{-\infty}^{\infty} G(x, z)\, e^{-ikx}\, dx, \tag{17a}$$

$$G(x, z) = \mathrm{Re}\left\{ \int_0^{\infty} \tilde{G}(k, z)\, e^{ikx}\, dk \right\}. \tag{17b}$$

2.2. Zeroth-order solutions

Taking the Fourier transform of (13) yields

$$U_0^2 \frac{\partial^2 \tilde{w}_0}{\partial z^2} + \tilde{w}_0 = \tilde{q}_0. \tag{18}$$

The non-dimensional basic-state wind is assumed to have a constant shear without a critical level

$$U_0 = 1 + \alpha z. \tag{19}$$

Here, the non-dimensional wind shear α is defined by $\alpha = \alpha^*/N$ where α^* is the dimensional wind shear. For convenience, we let $\beta = 1/\alpha$. The q_0 is assumed to have the same form as in CB, that is,

$$a_0 = \begin{cases} a_1(e^{-a_1 k} - e^{-a_2 k}) & \text{for } 0 \leqslant z \leqslant d \\ 0 & \text{for } z > d. \end{cases} \tag{20}$$

Here, a_1 and a_2 are the non-dimensional half-width of the forcing. Then, the general solution to (18) is

$$\tilde{w}_0(k, z) = A_0(k)(z + \beta)^{1/2 + iv} + B_0(k)(z + \beta)^{1/2 - iv} + \tilde{q}_0 \quad \text{for } 0 \leqslant z \leqslant d, \tag{21a}$$

$$\tilde{w}_0(k, z) = C_0(k)(z + \beta)^{1/2 + iv} + D_0(k)(z + \beta)^{1/2 - iv} \quad \text{for } z > d, \tag{21b}$$

where $v = \sqrt{\beta^2 - 1/4}$. Note that β^2 is the Richardson number since $\mathrm{Ri} = (N/\alpha^*)^2 = \beta^2$. In this study, we consider dynamically stable flow ($\mathrm{Ri} > 1/4$). The 4 unknown coefficients $A_0(k)$, $B_0(k)$, $C_0(k)$, and $D_0(k)$ can be determined by proper boundary and interface conditions. The flat bottom boundary condition requires $\tilde{w}_0 = 0$ at $z = 0$ and the upper radiation boundary condition for $U_0 > 0$ requires $D_0(k) = 0$ (Booker and Bretherton, 1967). At $z = d$, interface conditions that $\tilde{w}_0$ and $\partial \tilde{w}_0/\partial z$ are continuous are imposed.

Then, the zeroth-order solution in the wavenumber space is given by:

$$\tilde{w}_0(k, z) = \tilde{q}_0 \left\{ \left(\frac{1}{2} + \frac{1}{4iv} \right) (d+\beta)^{-1/2+iv} \times [\beta^{-2iv}(z+\beta)^{1/2+iv} - (z+\beta)^{1/2-iv}] - \beta^{-1/2-iv}(z+\beta)^{1/2+iv} + 1 \right\} \quad \text{for } 0 \leqslant z \leqslant d, \quad (22a)$$

$$\tilde{w}_0(k, z) = \tilde{q}_0 \left\{ \left(\frac{1}{2} + \frac{1}{4iv} \right) \times [\beta^{-2iv}(d+\beta)^{-1/2+iv} - (d+\beta)^{-1/2-iv}] - \beta^{-1/2-iv} + (d+\beta)^{-1/2+iv} \right\} (z+\beta)^{1/2+iv}, \quad \text{for } z > d, \quad (22b)$$

After taking the inverse Fourier transform of (22a) and (22b), the zeroth-order solution in the physical space can be obtained.

$$w_0(x, z) = X_1 \left[zs_1^{1/2} \left\{ \frac{1}{2} [\cos z_1 - \cos z_2] + \frac{1}{4v} [\sin z_1 - \sin z_2] \right\} - zs_2^{1/2} \cos z_3 + 1 \right] - X_2 \left[zs_1^{1/2} \left\{ \frac{1}{2} [\sin z_1 - \sin z_2] - \frac{1}{4v} [\cos z_1 - \cos z_2] \right\} - zs_2^{1/2} \sin z_3 \right] \quad \text{for } 0 \leqslant z \leqslant d, \quad (23a)$$

$$w_0(x, z) = X_1 \left[zs_1^{1/2} \left\{ \frac{1}{2} [\cos z_1 + \cos z_2] + \frac{1}{4v} [\sin z_1 + \sin z_2] \right\} - zs_2^{1/2} \cos z_3 \right] - X_2 \left[zs_1^{1/2} \left\{ \frac{1}{2} [\sin z_1 - \sin z_2] - \frac{1}{4v} [\cos z_1 - \cos z_2] \right\} - zs_2^{1/2} \sin z_3 \right] \quad \text{for } z > d, \quad (23b)$$

where

$$zs_1 = (z+\beta)/(d+\beta),$$
$$zs_2 = (z+\beta)/\beta,$$
$$z_1 = v \ln[(d+\beta)(z+\beta)/\beta^2],$$
$$z_2 = -v \ln(zs_1),$$
$$z_3 = v \ln(zs_2),$$
$$X_1 = \frac{a_1^2}{x^2+a_1^2} - \frac{a_1 a_2}{x^2+a_2^2},$$
$$X_2 = a_1 \left(\frac{x}{x^2+a_1^2} - \frac{x}{x^2+a_2^2} \right). \quad (24)$$

From the definition, the zeroth-order perturbation streamfunction can be obtained by integrating w_0 from $-\infty$ to x with respect to x.

$$\phi_0(x, z) = -X_3 \left[zs_1^{1/2} \left\{ \frac{1}{2} [\cos z_1 - \cos z_2] + \frac{1}{4v} [\sin z_1 - \sin z_2] \right\} - zs_2^{1/2} \cos z_3 + 1 \right] + X_4 \left[zs_1^{1/2} \left\{ \frac{1}{2} [\sin z_1 - \sin z_2] - \frac{1}{4v} [\cos z_1 - \cos z_2] \right\} - zs_2^{1/2} \sin z_3 \right] \quad \text{for } 0 \leqslant z \leqslant d, \quad (25a)$$

$$\phi_0(x, z) = -X_3 \left[zs_1^{1/2} \left\{ \frac{1}{2} [\cos z_1 + \cos z_2] + \frac{1}{4v} [\sin z_1 + \sin z_2] \right\} - zs_2^{1/2} \cos z_3 \right] + X_4 \left[zs_1^{1/2} \left\{ \frac{1}{2} [\sin z_1 - \sin z_2] - \frac{1}{4v} [\cos z_1 - \cos z_2] \right\} - zs_2^{1/2} \sin z_3 \right] \quad \text{for } z > d, \quad (25b)$$

where

$$X_3 = a_1 \left(\tan^{-1} \frac{x}{a_1} - \tan^{-1} \frac{x}{a_2} \right),$$
$$X_4 = \frac{a_1}{2} \ln \left(\frac{x^2+a_1^2}{x^2+a_2^2} \right). \quad (26)$$

The zeroth-order solution is proportional to zs_1

and zs_2 which increase with height. This implies that the solution will not be bounded as $z \to \infty$. This is due to the assumption that the basic-state wind increases linearly with height. In reality, the basic-state wind should be bounded at any height. In other words, the solutions (23) and (25) are valid where the assumption for the basic-state wind is valid. A similar problem could arise from the studies by Lin (1987) and Lin and Chun (1991).

The other zeroth-order variables u_0 and b_0 can be obtained using the perturbation streamfunction as follows.

$$u_0(x, z) = \frac{\partial \phi_0}{\partial z}, \tag{27}$$

$$b_0(x, z) = \frac{1}{U_0}\left(\phi_0 + \int_{-\infty}^{x} q_0 \, \mathrm{d}x\right). \tag{28}$$

2.3. 1st-order solutions

The 1st-order perturbation is forced by $F(x, z)$ which is determined by the zeroth-order perturbation. It follows that

$$F(x, z) = -\frac{1}{U_0}\left[2X_1 \frac{\partial \phi_0}{\partial z} + \frac{3}{U_0}\frac{\mathrm{d}U_0}{\mathrm{d}z}(\phi_0 + X_3)\frac{\partial \phi_0}{\partial x}\right]. \tag{29}$$

In the uniform flow case, $F(x, z) = -2X_1\, \partial\phi_0/\partial z$. The 2nd term on the right-hand side of (29) is related to the basic-state wind shear. This implies that even though the zeroth-order forcing q_0 is the same as both in the uniform flow case and in the shear case, the 1st-order perturbation is forced by additional forcing resulting from the wind shear. In addition, contrary to the uniform flow case, $F(x, z)$ exists above the forcing top height d. Note that X_1 and X_3 have values only below the forcing top height (zeroth-order forcing region $0 \leqslant z \leqslant d$). Therefore, it may be more convenient to write $F(x, z)$ in separate forms for each region:

$$F_1(x, z) = F(x, z) \qquad \text{for } 0 \leqslant z \leqslant d, \tag{30}$$

$$F_2(x, z) = -\frac{3}{U_0^2}\frac{\mathrm{d}U_0}{\mathrm{d}z}\phi_0\frac{\partial \phi_0}{\partial x} = -\frac{3\alpha}{U_0^2}\frac{\partial}{\partial x}\left(\frac{\phi_0^2}{2}\right) \qquad \text{for } z > d. \tag{31}$$

The forcings F_1 and F_2 are discontinuous at $z = d$ because of the discontinuity of X_1 and X_3 at $z = d$, even though solutions for the perturbation fields are forced to be continuous at $z = d$. The integration of F_1 from $x = -\infty$ to ∞ with respect to x is not zero as discussed in CB, while that of F_2 is zero, since it is in a perfect derivative. Therefore, there is no net forcing problem above the zeroth-order forcing region ($z > d$), and the solution may be bounded safely on far downstream side (Smith and Lin, 1982).

The governing equations of the 1st-order perturbation forced by F can be written in each region as

$$U_0^2\frac{\partial^2 \tilde{w}_1}{\partial z^2} + \tilde{w}_1 = \tilde{F}_1 \qquad \text{for } 0 \leqslant z \leqslant d, \tag{32a}$$

$$U_0^2\frac{\partial^2 \tilde{w}_1}{\partial z^2} + \tilde{w}_1 = \tilde{F}_2 \qquad \text{for } z > d. \tag{32b}$$

The general solutions to (32a) and (32b) are

$$\tilde{w}_1(k, z) = A_1(k)(z+\beta)^{1/2+iv} + B_1(k)(z+\beta)^{1/2-iv} + \tilde{w}_{1\mathrm{p}} \qquad \text{for } 0 \leqslant z \leqslant d, \tag{33a}$$

$$\tilde{w}_1(k, z) = C_1(k)(z+\beta)^{1/2+iv} + D_1(k)(z+\beta)^{1/2-iv} + \tilde{w}_{1\mathrm{p}} \qquad \text{for } z > d. \tag{33b}$$

Here, $\tilde{w}_{1\mathrm{p}}$ is the particular solution given by

$$\tilde{w}_{1\mathrm{p}}(k, z) = \alpha_1(k, z)(z+\beta)^{1/2+iv} + \alpha_2(k, z)(z+\beta)^{1/2-iv}, \tag{34}$$

where

$$\alpha_1(k, z) = -\int \frac{\tilde{F}(k, z)(z+\beta)^{1/2-iv}}{W[(z+\beta)^{1/2+iv}, (z+\beta)^{1/2-iv}]}\,\mathrm{d}z, \tag{35a}$$

$$\alpha_2(k, z) = \int \frac{\tilde{F}(k, z)(z+\beta)^{1/2+iv}}{W[(z+\beta)^{1/2+iv}, (z+\beta)^{1/2-iv}]}\,\mathrm{d}z. \tag{35b}$$

Here, the symbol W is the Wronskian defined by $W(C, D) = C(\mathrm{d}D/\mathrm{d}z) - D(\mathrm{d}C/\mathrm{d}z)$. Because $W[(z+\beta)^{1/2+iv}, (z+\beta)^{1/2-iv}] = -2iv$, the particular solution becomes

$$\tilde{w}_{1\mathrm{p}}(k, z) = -\frac{i}{2\pi v}(z+\beta)^{1/2+iv}\int_{-\infty}^{\infty} S(x, z)\,\mathrm{e}^{-ikx}\,\mathrm{d}x + \frac{i}{2\pi v}(z+\beta)^{1/2-iv}\int_{-\infty}^{\infty} T(x, z)\,\mathrm{e}^{-ikx}\,\mathrm{d}x, \tag{36}$$

where

$$S(x, z) = \int F(x, z)(z+\beta)^{1/2-i\nu}\,\mathrm{d}z, \tag{37a}$$

$$T(x, z) = \int F(x, z)(z+\beta)^{1/2+i\nu}\,\mathrm{d}z. \tag{37b}$$

By the definition of the Fourier transform, (36) is equivalent to

$$\tilde{w}_{1p}(k, z) = -\frac{i}{2\nu}(z+\beta)^{1/2+i\nu}\tilde{S}(k, z) + \frac{i}{2\nu}(z+\beta)^{1/2-i\nu}\tilde{T}(k, z). \tag{38}$$

since $S(x, z)$ and $T(x, z)$ are different for each region, $\tilde{S}(k, z)$ and $\tilde{T}(k, z)$ are discontinuous at $z = d$. As was done for the zeroth-order solution, the lower boundary condition of $\tilde{w}_1 = 0$ at $z = 0$, the upper radiation boundary condition $[D_1(k) = 0]$, and the interface conditions of the continuity of $\tilde{w}_1$ and $\partial\tilde{w}_1/\partial z$ at $z = d$ are imposed to determine the 4 unknown coefficients $A_1(k)$, $B_1(k)$, $C_1(k)$, and $D_1(k)$ in (33a) and (33b). After relatively complicated manipulations, the solution for the first-order perturbation vertical velocity can be obtained by:

$$\begin{aligned}\tilde{w}_1(k, z) &= \frac{i}{2\nu}[\tilde{S}_1(k, 0) - \beta^{-2i\nu}\tilde{T}_1(k, 0)](z+\beta)^{1/2+i\nu} \\ &\quad + \frac{i}{2\nu}\beta^{-2i\nu}\Big\{[\tilde{T}_1(k, d) - \tilde{T}_2(k, d)] \\ &\quad - \frac{i}{2\nu}(d+\beta)^{1/2+i\nu}\left[\frac{\partial\tilde{S}_1}{\partial z}(k, d) - \frac{\partial\tilde{S}_2}{\partial z}(k, d)\right] \\ &\quad + \frac{i}{2\nu}(d+\beta)\left[\frac{\partial\tilde{T}_1}{\partial z}(k, d) - \frac{\partial\tilde{T}_2}{\partial z}(k, d)\right]\Big\} \\ &\quad \times [(z+\beta)^{1/2+i\nu} - \beta^{2i\nu}(z+\beta)^{1/2-i\nu}] \\ &\quad - \frac{i}{2\nu}[(z+\beta)^{1/2+i\nu}\tilde{S}_1(k, z) \\ &\quad - (z+\beta)^{1/2-i\nu}\tilde{T}_1(k, z)], \qquad \text{for } 0 \leqslant z \leqslant d, \end{aligned} \tag{39a}$$

$$\begin{aligned}\tilde{w}_1(k, z) &= \frac{i}{2\nu}\Big\{\tilde{S}_1(k, 0) - \beta^{-2i\nu}\tilde{T}_1(k, 0) \\ &\quad - [\tilde{S}_1(k, d) - \tilde{S}_2(k, d)] + \beta^{-2i\nu}[\tilde{T}_1(k, d) \\ &\quad - \tilde{T}_2(k, d)] - \frac{i}{2\nu}(d+\beta)[\beta^{-2i\nu}(d+\beta)^{2i\nu} - 1] \\ &\quad \times \left[\frac{\partial\tilde{S}_1}{\partial z}(k, d) - \frac{\partial\tilde{S}_2}{\partial z}(k, d)\right] \\ &\quad + \frac{i}{2\nu}(d+\beta)[\beta^{-2i\nu} - (d+\beta)^{-2i\nu}] \\ &\quad \times \left[\frac{\partial\tilde{T}_1}{\partial z}(k, d) - \frac{\partial\tilde{T}_2}{\partial z}(k, d)\right]\Big\}(z+\beta)^{1/2+i\nu} \\ &\quad - \frac{i}{2\nu}[(z+\beta)^{1/2+i\nu}\tilde{S}_2(k, z) \\ &\quad - (z+\beta)^{1/2-i\nu}\tilde{T}_2(k, z)], \qquad \text{for } z > d. \end{aligned} \tag{39b}$$

Here, the subscripts 1 and 2 in $\tilde{S}(k, z)$ and $\tilde{T}(k, z)$ denote $\tilde{S}(k, z)$ and $\tilde{T}(k, z)$ in the regions of $0 \leqslant z \leqslant d$ and $z > d$, respectively. Note that all the variables of $F(x, z)$ in (29) are continuous at $z = d$ except for the specified forcing including X_1 and X_3. The only difference in $\tilde{S}(k, z)$, $\tilde{T}(k, z)$, $\partial\tilde{S}(k, z)/\partial z$, and $\partial\tilde{T}(k, z)/\partial z$ between 2 regions is the specified forcing term. As mentioned in the zeroth-order solution, the 1st-order solution also includes zs_1 and zs_2 terms implicitly. In addition, the 1st-order solution for $z > d$ includes $\tilde{S}_2(k, z)$ and $\tilde{T}_2(k, z)$, which also include the zs_1 and zs_2 terms. However, because $\tilde{S}_2(k, z)$ and $\tilde{T}_2(k, z)$, are proportional to α/U_0^2 [(31) and (37)], they may be bounded safely as $z \to \infty$.

To get the 1st-order perturbation vertical velocity field in the physical space, first $S(x, z)$ and $T(x, z)$ are numerically evaluated by solving the matrix system, as analytical integrations appear to be fairly complicated to perform ((37a) and (37b)). Differentiations of $S(x, z)$ and $T(x, z)$ with respect to z give, respectively,

$$\frac{\partial S}{\partial z} = F(x, z)(z+\beta)^{1/2-i\nu}, \tag{40a}$$

$$\frac{\partial T}{\partial z} = F(x, z)(z+\beta)^{1/2+i\nu}. \tag{40b}$$

The 4th-order finite difference equations of (40a) and (40b) in the z-direction (subscript j) in each region are given by

$$H_{j+2} - 8H_{j+1} + 8H_{j-1} - H_{j-2} = 12\Delta z h_j, \tag{41}$$

where H and h denote $S(x, z)$ (or $T(x, z)$) and $F(x, z)(z+\beta)^{1/2-i\nu}$ (or $F(x, z)(z+\beta)^{1/2+i\nu}$), and Δz

is the vertical grid interval. $\partial S(x,z)/\partial z$ and $\partial T(x,z)/\partial z$ are analytically evaluated using (40a) and (40b). Then $S(x,z)$, $T(x,z)$, $\partial S(x,z)/\partial z$, and $\partial T(x,z)/\partial z$ are forward-transformed $(x \to k)$ to get $\tilde{S}(k,z)$, $\tilde{T}(k,z)$, $\partial \tilde{S}(k,z)/\partial z$, and $\partial \tilde{T}(k,z)/\partial z$, and from (39a) and (39b), $\tilde{w}_1(k,z)$ is evaluated. Finally, $\tilde{w}_1(k,z)$ is backward-transformed $(k \to \infty)$ to obtain $w_1(x,z)$. A fast Fourier transform (FFT) algorithm is employed to perform the forward- and backward-transforms. For the computations, the number of horizontal wavenumbers is specified as 512 over the horizontal domain size of 51.1 and the vertical domain size in 10 with a vertical grid interval of 0.05. The non-dimensional length scales a_1 and a_2 in (20) are set to 1 and 5, respectively.

3. Energy and momentum flux argument

From the zeroth-order horizontal momentum, thermodynamic energy, mass continuity, and hydrostatic equations, the zeroth-order wave energy equation can be derived as follows.

$$\frac{\partial}{\partial x}[U_0 E_0 + \pi_0 u_0] + \frac{\partial}{\partial z}(\pi_0 w_0) = q_0 b_0 - \alpha u_0 w_0. \tag{42}$$

Here, E_0 is the zeroth-order total wave energy defined by $(u_0^2 + b_0^2)/2$ and π_0 the zeroth-order perturbation kinematic pressure. This is identical to the dimensional form in Lin (1987). In contrast to the uniform basic-state wind case in CB, the vertical wind shear can be a wave energy source. Because the zeroth-order momentum flux $u_0 w_0$ is negative for the vertically propagating waves, the 2nd term on the right-hand side of (42) is positive for positive vertical wind shear ($\alpha > 0$), as in the present case. This implies that the wave can extract energy from the mean flow with vertical shear. Since the zeroth-order energy argument is already given in several studies (Lin, 1987; Chun, 1991; Baik, 1992), our interest here lies in connection between the zeroth-order and 1st-order wave energy.

Using the 1st-order governing equations, the 1st-order wave energy equation can be obtained from:

$$\frac{\partial}{\partial x}[U_0 E_1 + \pi_1 u_1] + \frac{\partial}{\partial z}(\pi_1 w_1) = -\frac{u_1}{U_0}\left[\frac{\partial}{\partial x}(U_0 E_0) - b_0 q_0\right] + \frac{b_1 F}{2} - \alpha\left[u_1 w_1 + \frac{b_1 w_0 b_0}{2U_0}\right]. \tag{43}$$

Here, E_1 is the 1st-order total wave energy defined by $E_1 = (u_1^2 + b_1^2)/2$ and π_1 the 1st-order perturbation kinematic pressure. The 1st 3 terms on the right-hand side of (43) are equivalent to those in the uniform basic-state wind case in CB, while the last 2 terms in (43) are related to the vertical shear of the basic-state wind. Therefore, (43) is a generalized form of (47) in CB. The 1st term in the last bracket is the 1st-order vertical momentum flux which should be negative for the wave energy to propagate upward (Booker and Bretherton, 1967). Multiplying $(U_0 u_1 + \pi_1)$ with the 1st-order horizontal momentum equation and integrating from $x = -\infty$ to ∞ with respect to x yields the following vertical wave energy equation:

$$\int_{-\infty}^{\infty} \pi_1 w_1 \, dx = -U_0 \int_{-\infty}^{\infty} u_1 w_1 \, dx + \frac{1}{\alpha}\int_{-\infty}^{\infty} (U_0 u_1 + \pi_1) J\left(\phi_0, \frac{\partial \phi_0}{\partial z}\right) dx. \tag{44}$$

The 2nd integrand in the right-hand side of (44) represents wave interaction between the zeroth-order and 1st-order perturbations. Integrating (43) from $x = -\infty$ to ∞ with respect to x and differentiating (44) with respect to z gives the following equation of the vertical variation of the momentum flux:

$$\frac{d}{dz}\int_{-\infty}^{\infty} u_1 w_1 \, dx = -\frac{1}{U_0}\int_{-\infty}^{\infty} \frac{b_1 F}{2} dx + \frac{\alpha}{2U_0^2}\int_{-\infty}^{\infty} b_1 w_0 b_0 \, dx + \frac{1}{\alpha}\frac{d}{dz}\int_{-\infty}^{\infty} u_1 J\left(\phi_0, \frac{\partial \phi_0}{\partial z}\right) dx + \frac{1}{\alpha U_0}\frac{d}{dz}\int_{-\infty}^{\infty} \pi_1 J\left(\phi_0, \frac{\partial \phi_0}{\partial z}\right) dx. \tag{45}$$

Note that (43)–(45) are valid only when there is no critical level ($U_0 \neq 0$). The 1st term on the right-hand side of (45) represents the source of the momentum flux divergence by diabtic forcing to the 1st-order perturbation induced by the Jacobian of the zeroth-order perturbation. There is a vertical convergence of the momentum flux when the buoyancy perturbation in the heating region is positive for the case of $U_0 > 0$. The 2nd term represents a connection between the zeroth-order and 1st-order perturbations. The 3rd and 4th terms also represent connections between the zeroth-order and 1st-order perturbations through $J(\phi_0, \partial\phi_0/\partial z)$.

Unlike the zeroth-order (linear) perturbation, there exists a vertical covnergence of the momentum flux both inside and outside the specified forcing region. The vertical convergence of the horizontally-averaged momentum flux is especially important because it can influence the large-scale mean motion in terms of gravity wave drag. It is well-known that the observed zonal mean zonal wind and temperature are simulated in general circulation models (GCMs) when the gravity wave drag parametrization is included. In most theoretical (Lindzen, 1981; Pierrehumbert, 1986) and GCM (Palmer et al., 1986; McFarlane, 1987) studies of gravity wave drag effects on the large-scale atmospheric motion, the mountain has been considered as a source of gravity waves. For the linear, steady-state, inviscid mountain waves, the momentum flux is constant with height without a critical level (Eliassen and Palm, 1960). Therefore, the contribution of gravity waves to the large-scale mean flow is possible only where wave braking occurs. However, for the thermally-induced gravity waves, there exists a vertical convergence of the momentum flux wherever the thermal forcing exists even for the linear, steady-state, inviscid flow without a wave breaking. If the flow is non-linear, even weakly non-linear, the vertical convergence of the momentum flux exists outside the thermal forcing region by the vertical wind shear through the wave–wave interaction (zeroth-order and 1st-order perturbation interaction for the weakly nonlinear case). During summer-time when the surface wind is weak and stability is small compared to winter-time, the contribution of mountain waves for gravity wave drag becomes small. However, the thermal forcing by the cumulus convection cannot be ignored for the gravity wave source. Furthermore, in the tropical region where cumulus convection is persistent, gravity waves induced by tall cumulus impinging the stable lower stratosphere may influence the large-scale mean flow (Fovell et al., 1992).

In general, there is no actual non-linear interaction between the mean flow and waves for the weakly non-linear approach using the perturbation expansion. It is much like a one-way interaction from lower to higher order, such that the mean flow influences the zeroth-order wave and the zeroth-order wave influences the 1st-order wave. However, if we consider a time-dependent problem, basic-state wind itself can be changed with time where the vertical convergence/divergence of the wave momentum flux exists as in the present case. In this sense, steady-state response and asymptotic behavior of the transient response as $t \to \infty$ for a given structure of the basic-state wind may not be the same. This may be because the basic-state wind for the steady-state case should be different from that for the transient case, since basic-state wind itself can be changed by wave momentum flux. Therefore, the basic-state wind in the present study is better considered as a steady-state ($t \to \infty$) basic state wind.

4. Results and discussion

Figure 1 shows the specified heating q_0, the forcing F_1 to the 1st-order equation in the specified forcing region, and the forcing F_2 to the 1st-order equation above the specified forcing region. The heating depth and the vertical wind shear α are specified as 1 and 0.1, respectively. This value of α corresponds to $10\ \mathrm{ms}^{-1}$ wind speed difference between the surface and 10 km height with a typical value of $N = 0.01\ \mathrm{s}^{-1}$. As in the uniform basic-wind case (CB), F_1 represents cooling in the specified heating region. The F_1 field shows an upstream phase tilt because the zeroth-order solution itself has an upstream phase tilt by the constraint of upward energy propagation. Unlike CB, however, the forcing to the 1st-order perturbation above the specified heating region is non-zero because of the vertical wind shear [(31)]. The F_2 field shows wave type, and its magnitude is one order smaller than that of q_0 for F_1 in this case. Horizontally, F_2 represents cooling on the upstream side and heating on the downstream side just above the specified forcing and reverses its forcing type periodically with height. As men-

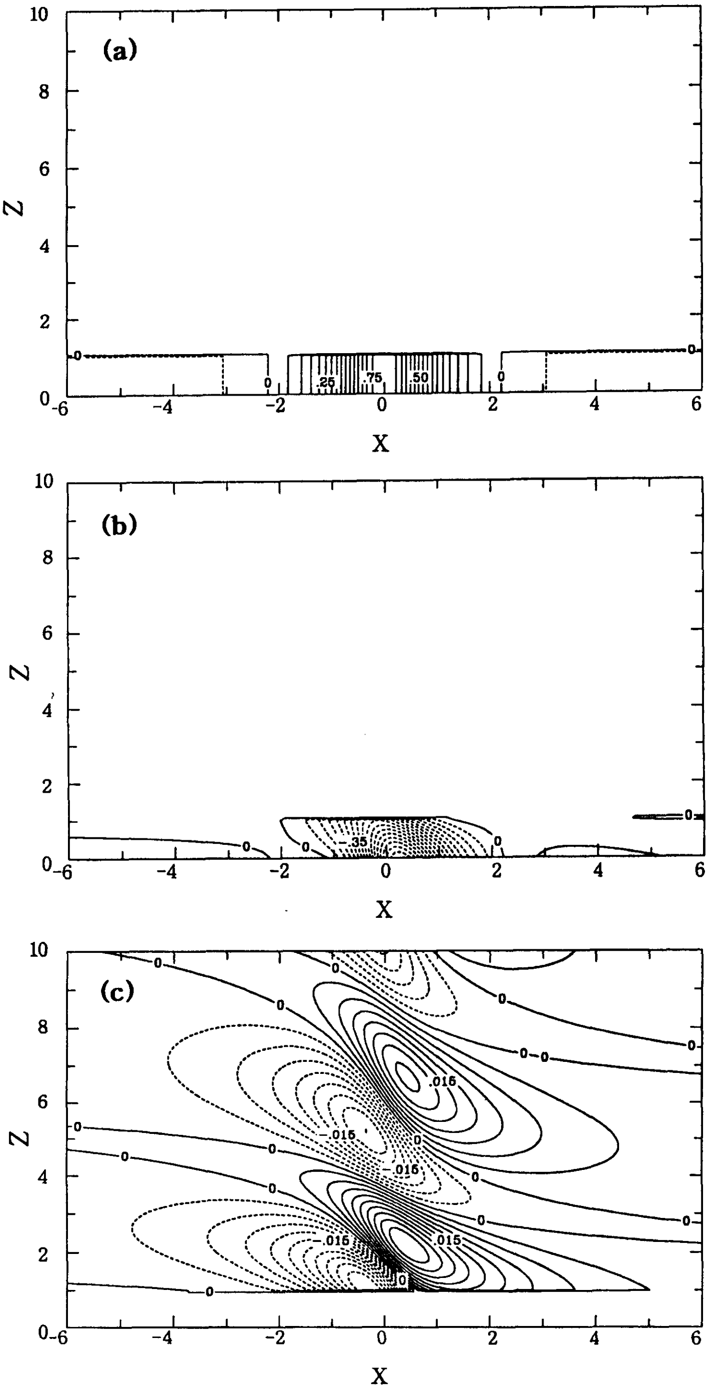

Fig. 1. The fields of (a) the specified heating q_0, (b) the forcing F_1 to the 1st-order equation below d, and (c) the forcing F_2 to the 1st-order equation above d for the case of $d = 1$ and $\alpha = 0.1$. Contour intervals in (a), (b), and (c) are 0.05, 0.07, and 0.003, respectively.

tioned earlier, an integration of F_2 from $x = -\infty$ to ∞ with respect to x is zero. The forcings F_1 and F_2 are discontinuous at $z = d$, since F_1 includes a q_0 term which is discontinuous at $z = d$. The vertical structure of F_2 is related to that of the zeroth-order perturbation. Because the non-dimensional vertical wavelength of dominant gravity wave ($\lambda_z = \lambda_z^*/(U_c/N) = (2\pi U^*/N)/(U_c/N) = 2\pi(1 + \alpha z)$, where the superscript * denotes dimensional) depends on the basic-state wind, an infinite number of vertical wavelengths are possible for the present shear flow case. The vertical wavelength increases with height and increasing wind shear.

The zeroth-order and 1st-order vertical velocity fields for the cases of $d = 1$ and $\alpha = 0.1$ are shown in Fig. 2. The 2 fields almost reverse their signs while the maximum and minimum values remain slightly different from each other. The downward motion on the upstream side of the heating in the zeroth-order perturbation field is one of important findings of the linear analytic studies. The negative-phase relationship between the heating and the induced vertical motion in the vicinity of the forcing center, results from the mean wind advection (Smith and Lin, 1982; Lin and Smith, 1986). On the other hand, there exists an upward motion in the 1st-order perturbation field at almost the same place where the downward motion exists in the zeroth-order perturbation field. This response is somewhat expected because the main forcing to the first-order perturbation F_1 is a localized cooling located at the place where the specified heating exists as shown in Fig. 1b. Note that F_1 represents cooling near the surface regardless of the specified forcing type (heating or cooling) as pointed out in CB. Therefore, a weakly non-linear response of a stably stratified flow to specified heating is similar to the linear response to both heating and cooling. However, the cooling in this study is not specified as in Lin and Chun (1991) but induced by the zeroth-order perturbation. Thus, F_1 is neither horizontally symmetric nor vertically uniform as in q_0 but tilted upstream by the upstream tilted zeroth-order perturbation.

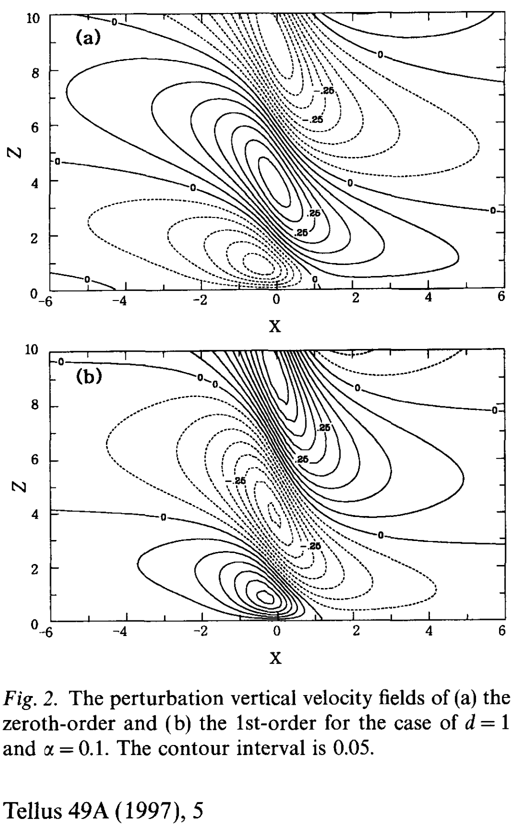

Fig. 2. The perturbation vertical velocity fields of (a) the zeroth-order and (b) the 1st-order for the case of $d = 1$ and $\alpha = 0.1$. The contour interval is 0.05.

Fig. 3 shows the zeroth-order and 1st-order vertical velocity fields for the case of $d = 1$ and $\alpha = 0.2$. Because the vertical wind shear is doubled

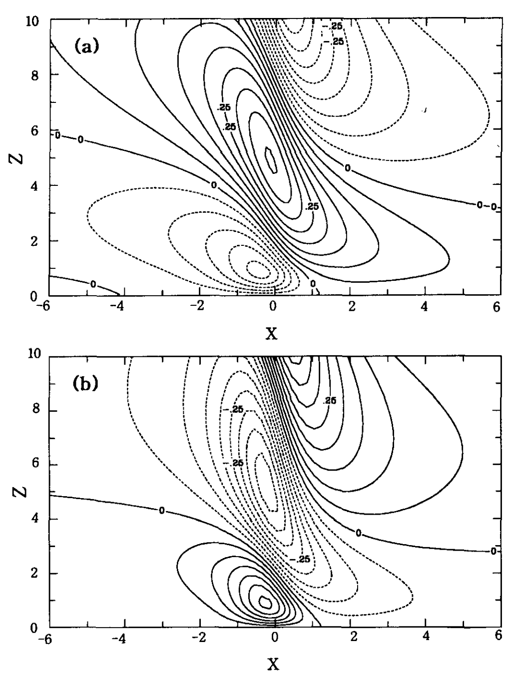

Fig. 3. As in Fig. 2 except for $\alpha = 0.2$.

compared with that in Fig. 2, both the vertical wavelength and the slope of phase tilt increase. In comparison with the $\alpha = 0.1$ case, the zeroth-order maximum vertical velocity increases slightly, while the 1st-order maximum vertical velocity decreases slightly simply because the w_1 maximum is located above the plotting domain due to the increased vertical wavelength. Within the vertical domain considered in this study, the magnitude of the 1st-order perturbation can be alternatively checked by the 1st-order minimum vertical velocity.

Fig. 4a shows the domain maximum zeroth-order vertical velocity and minimum 1st-order vertical velocity as a function of the vertical wind shear. The maximum w_0 increases with increasing wind shear because waves can extract energy from the mean flow with wind shear. Note that the domain maximum w_0 exists above the forcing region where the only source of wave energy comes from the basic-state wind shear (42). However, the magnitude of the minimum w_1 remains little changed with increasing wind shear. This seems to be related to the magnitude of F_2 which varies with wind shear. Fig. 4b shows the domain maximum absolute magnitude of F_2 as a function of the vertical wind shear. Because F_2 is determined by the multiple of $\alpha/(1+\alpha z)^2$ and $\partial(\phi_0^2)/\partial x$, the vertical wind shear is directly related to $\alpha/(1+\alpha z)^2$ and indirectly to $\partial(\phi_0^2)/\partial x$. The increasing vertical wind shear reduces the value of $\alpha/(1+\alpha z)^2$ term for a given z above $z = d$ and increases the value of the $\partial(\phi_0^2)/\partial x$ term. Since α is non-linearly related to both the terms in F_2, the absolute magnitude of F_2 does not monotonously increase or decrease with α.

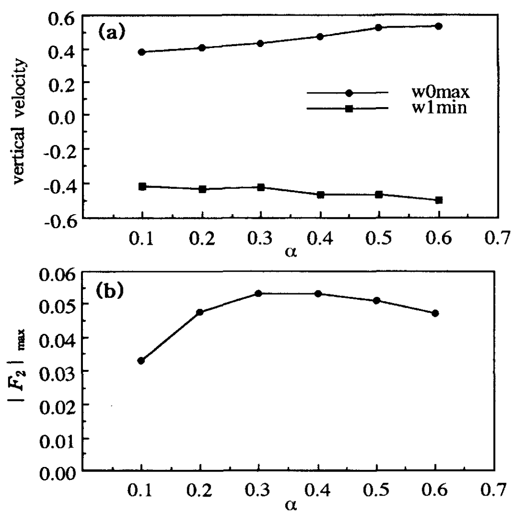

Fig. 4. (a) The domain maximum zeroth-order perturbation vertical velocity ($w_{0\max}$) and the domain minimum 1st-order perturbation vertical velocity ($w_{1\min}$) and (b) the domain maximum absolute magnitude of F_2 ($|F_2|_{\max}$) as a function of α.

Fig. 5 shows the zeroth-order and 1st-order horizontal velocity perturbations for the case of $d = 1$ and $\alpha = 0.2$. In the zeroth-order perturbation field, there exist a low-level divergence (convergence) on the upstream (downstream) side of the specified heating below $z = d$, and this pattern reverses periodically with height above $z = d$. This divergence (convergence) is responsible for the downward (upward) motion as shown in Fig. 3a. One the other hand, there is a strong convergence at the surface from the upstream to the center of the heating in the 1st-order perturbation field. This convergence produces upward motion on the upstream side of the specified heating through the mass continuity equation as shown in Fig. 3b.

The domain maximum zeroth-order perturbation horizontal velocity and minimum 1st-order perturbation horizontal velocity are located at the surface on the downstream side of the specified forcing. The magnitudes of both the zeroth-order and 1st-order perturbation horizontal velocities for the $\alpha = 0.2$ case are smaller in the lower layer ($z \leqslant d$) than those corresponding to the $\alpha = 0.1$ case (not shown here). Fig. 6a shows the domain maximum u_0 and minimum u_1 as a function of the vertical wind shear. The magnitudes of both the maximum u_0 and minimum u_1 decrease as the wind shear increases. When we consider that the maximum w_0 increases with increasing wind shear, decreasing maximum u_0 with increasing wind shear appears to be inconsistent at the first glance. However, this may be explained by a vorticity concept. Since the vorticity in the present system is given by $\partial u/\partial z$, the basic-state wind can produce vorticity as much as α for the constant shear flow. On the other hand, the localized heating can produce negative (positive) vorticity on the upstream (downstream) side of the heating (Rotunno et al., 1988). Therefore, when the inflow has a stronger shear, a larger part of the specified heating should be used to compensate for the positive vorticity induced by the positive basic-state wind shear. Consequently, the effective heating to produce the perturbation horizontal vel-

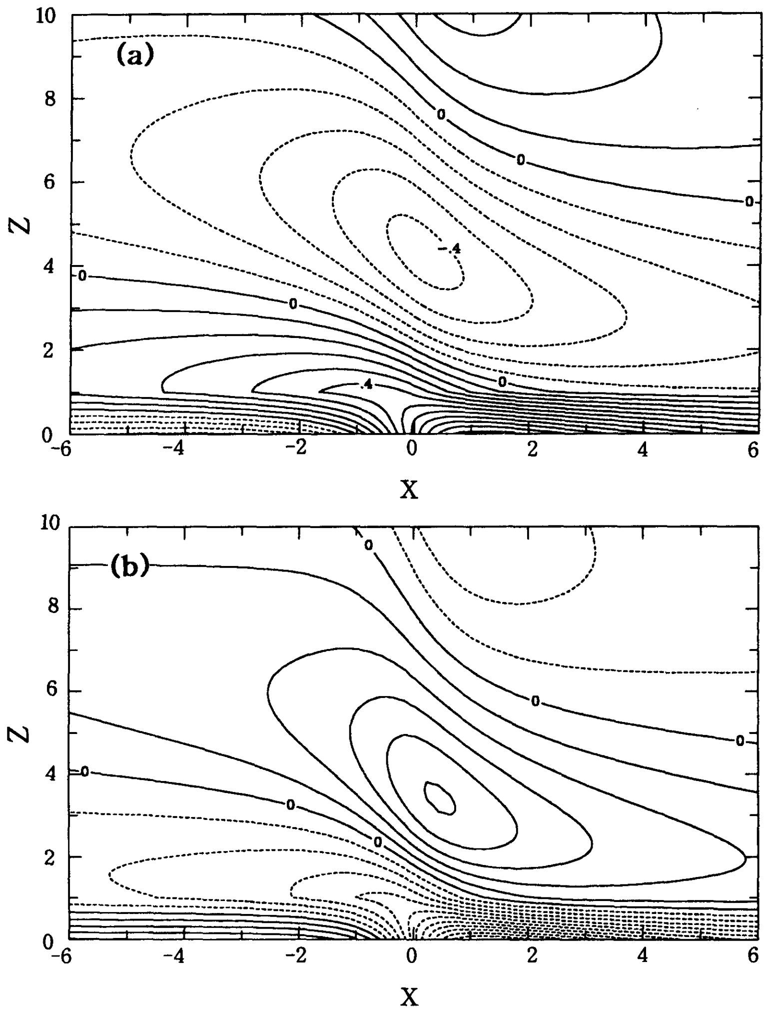

Fig. 5. The perturbation horizontal velocity fields of (a) the zeroth-order and (b) the 1st-order for the case of $d = 1$ and $\alpha = 0.2$. Contour intervals in (a) and (b) are 0.08 and 0.07, respectively.

ocity becomes smaller for stronger shear case. Thus, the magnitudes of the perturbation horizontal velocities on both upstream and downstream sides become smaller for stronger shear case. Lin and Chun (1991) presented a similar result that the density current speed propagating upstream can be reduced by the basic-state wind in the present case are reversed compared to those in Lin and Chun (1991), the positive wind shears for both the cases reduce the effective forcing to produce the perturbation horizontal velocity.

For the 1st-order perturbation horizontal velocity, the minimum u_1 decreases as the vertical wind shear increases. This can be explained in 2 ways. Firstly, as in the zeroth-order case, increasing wind shear reduces the effective forcing to the 1st-order perturbation by compensating for the positive vorticity induced by the basic-state wind shear. Secondly, F_1 itself depends on the basic-state wind shear directly through the basic-state wind and indirectly through the zeroth-order perturbation (29). As shown in Fig. 6b, the magnitude of the minimum F_1 decreases monotonously as the wind shear increases.

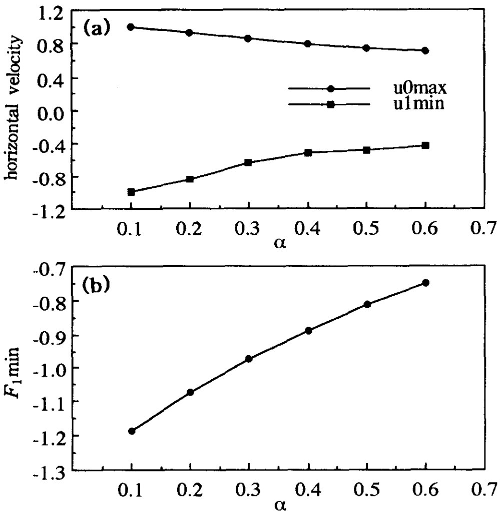

Fig. 6. (a) the domain maximum zeroth-order perturbation horizontal velocity ($u_{0\max}$) and the domain minimum 1st-order perturbation horizontal velocity ($u_{1\min}$) and (b) the domain minimum F_1 ($F_{1\min}$) as a function of α.

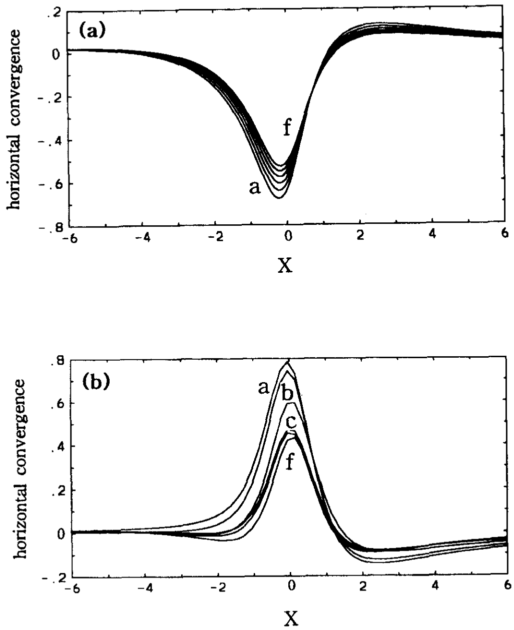

Fig. 7. The horizontal convergence ($-\partial u/\partial x$) of (a) the zeroth-order and (b) the 1st-order for the case of $d = 1$ with different vertical wind shears. Curves (a) and (f) in (7a) represent cases with $\alpha = 0.1$ and 0.6, respectively. Curves a, b, c, and f in (7b) represent cases with $\alpha = 0.1$, 0.2, 0.3, and 0.6, respectively.

In CB, the main non-linearity effect of the weakly non-linear response of the stably stratified uniform flow to specified heating, is the low-level convergence and resultant upward motion on the upstream side of the heating. In the present study, emphasis is put on the effects of the basic-state wind shear on the weakly non-linear response. Effects of the vertical wind shear on the horizontal convergence both by the zeroth-order and 1st-order perturbations at the surface with different wind shears are shown in Fig. 7a and 7b, respectively. Wind shears considered here are in the range of 0.1–0.6 with a 0.1 increment. These values of the wind shear correspond to the Richardson numbers of $2.87 \leqslant \mathrm{Ri} \leqslant 100$. For the clarity of the figures, only limited number of labels are included. Curves a and f in Fig. 7a represent cases with $\alpha =$ 0.1 and 0.6, respectively. In Fig. 7b, curves a, b, c, and f represent cases with $\alpha = 0.1$, 0.2, 0.3, and 0.6, respectively. There exist horizontal divergences for the zeroth-order perturbation from upstream to the center of the specified heating and weak convergence on the downstream side. The magnitudes of these divergence and convergence decrease with increasing wind shear. Horizontally, the divergence pattern is more symmetric with respect to $x = 0$ as the wind shear becomes stronger. This is also true for the convergence and divergence of the 1st-order perturbation. In contrast to the weak shear case, there exists weak divergences both on the upstream ($x = -2$) and downstream sides of the heating for the stronger shear case. Thus, as the wind shear increases, the magnitudes of the divergence (convergence) on the upstream side and the convergence (divergence) on the downstream side of the heating for the zeroth-order (1st-order) perturbation, decrease.

Overall, the wind shear decreases the magnitudes of the perturbations for both the zeroth-order and 1st-order in the lower layer. This can be seen from the momentum flux profiles. Fig. 8 shows the momentum flux defined by $\int_{-\infty}^{\infty} uw \, \mathrm{d}x$ for the zeroth-order and 1st-order with different vertical wind shears. As in Fig. 7, only a limited number of labels are included for the clarity of the figures. Curves a, b, c, and f represent cases with $\alpha = 0.1$, 0.2, 0.3, and 0.6, respectively. The momentum flux for the zeroth-order perturbation above the specified heating region is constant with

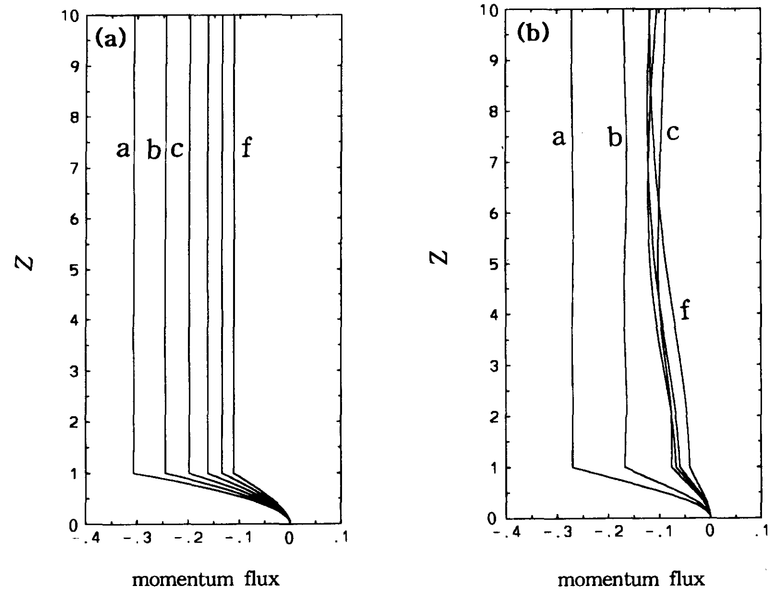

Fig. 8. The momentum flux profiles of (a) the zeroth-order and (b) the 1st-order for the cases of $d = 1$ with different vertical wind shears. Curves a, b, c, and f represent cases with $\alpha = 0.1$, 0.2, 0.3, and 0.6, respectively.

height. Even though the maximum w_0 above the heating height increases with increasing wind shear, the horizontal integration of $u_0 w_0$ becomes smaller for stronger wind shear case. In this study, the momentum flux is integrated numerically over a horizontal domain size of 51.1. This horizontal domain size appears to be large enough to eliminate periodic boundary condition for the Fourier transform. The magnitude of the momentum flux in the specified heating region decreases monotonously with increasing wind shear for both the zeroth-order and 1st-order perturbations. Above the specified heating region, there exists a vertical convergence or divergence of the momentum flux for the 1st-order perturbation. This is obvious for the stronger wind shear case. It appears that the vertical variation of the momentum flux is different with height for a given wind shear and different with wind shear for a given height due to the vertical wavelength.

5. Summary and conclusions

A weakly non-linear response of a stably stratified shear flow to the specified heating was investigated analytically. Emphasis was put on the effects of the basic-state wind shear (a) on the weakly non-linear response compared to a similar study by Chun and Baik (1994) in the uniform basic-state wind case. A two-dimensional (x–z plane), steady-state, hydrostatic, non-rotating, inviscid, Boussinesq flow system in a shear flow with diabatic heating was considered. The basic-state wind was assumed to have a constant shear without a critical level. The diabatic heating was prescribed to be uniform from the surface to a certain height vertically and bell-shaped horizontally.

Using the perturbation expansion in small values of the nonlinearity factor of the thermally-induced waves, the equations of the lowest 2 powers (zeroth-order (linear) and 1st-order (largest weakly nonlinear)) were solved. The zeroth-order solution was obtained analytically in the physical domain, while the 1st-order solution was obtained analytically in the wavenumber domain and transformed back to the physical domain using the FFT algorithm. The non-dimensional heating depth (d) or inverse of the Froude number associated with the diabatic forcing (Smith and Lin, 1982) was fixed as 1, and the range of the vertical wind shear was in the range 0.1–0.6. Under the given d, the forcing to the 1st-order perturbation F induced by the Jacobian of the zeroth-order perturbation represents cooling in the specified heating region which decreases with increasing wind shear. Unlike the uniform basic-state wind case, the forcing to the 1st-order perturbation above the specified heating region (F_2) has a non-zero value by the basic-state wind shear. The F_2 field shows a wave-type structure which is one order smaller in magnitude than F in the forcing region (F_1). The magnitude of F_2 varies irregularly with wind shear because it is non-linearly related to the wind shear.

The zeroth-order maximum vertical velocity above d increases with increasing vertical wind shear by extracting energy from the mean flow. On the other hand, the corresponding 1st-order vertical velocity perturbation varies irregularly with wind shear because of the variation of F_2 by the wind shear. The maximum perturbation horizontal velocity in the lower layer ($z < d$) decreases for both the zeroth-order and 1st-order perturbations with increasing wind shear. For the zeroth-order perturbation, this is because the effective heating used to produce the perturbation horizontal velocity is reduced by compensating for the positive vorticity induced by the positive basic-state wind shear. For the 1st-order horizontal velocity perturbation, this is because of both the effective forcing reduced by compensating for the basic-state wind shear, and the magnitude of F_1 itself decreasing with wind shear. The magnitude of the horizontal divergence (convergence) for the zeroth-order (1st-order) perturbation at the surface of the upstream (upstream or center) decreases with increasing wind shear and the structure becomes more symmetric with respect to the center of the heating ($x = 0$). As the wind shear is strong enough, there is a weak divergence for the 1st-order perturbation on the upstream side of the heating.

The energy equation for the 1st-order perturbation with the basic-state wind shear showed that there is a vertical convergence of the momentum flux in the specified heating region for both the zeroth-order and 1st-order perturbations, decreasing with increasing wind shear. In addition, unlike the uniform basic-state wind case, there is a vertical convergence/divergence of the momentum flux for the 1st-order perturbation above the specified heating region. The magnitude of the vertical convergence/divergence varies irregularly with wind shear, because it depends on the vertical wavelength which varies itself with wind shear. The existence of the vertical convergence/divergence of the momentum flux is important to the large-scale mean flow as the subgrid scale gravity wave drag, suggesting that the gravity wave drag induced by the thermal forcing cannot be ignored for certain conditions where the diabatic forcing is dominant.

Even though the behavior and magnitude of each order perturbation are independent of the non-linearity parameter in general ϕ_0 and ϕ_1 in this study are not totally independent of μ because μ includes N which can control the Richardson number. However, if we consider increase/decrease of μ based upon the increase/decrease of heating rate for given N and U_c, ϕ_0 and ϕ_1 are totally independent of μ. Rather, ϕ_0 and ϕ_1 depend on the non-dimensional heating depth d which is the inverse of the Froude number. Note that above-mentioned results are based on the cases with $d = 1$ and $0.1 \leqslant \alpha \leqslant 0.6$. Therefore, any conclusions in this study are a subset of those for the full parameter domain of d and α. However, this research provides an insight into how the non-linearity affects a stably stratified shear flow to specified heating for different shears, even though there may exist fundamental differences between the weakly non-linear response and the fully non-linear response as discussed in Baik and Chun (1996).

6. Acknowledgements

The author is very grateful to Jong-Jin Baik for providing valuable comments on this study.

REFERENCES

Baik, J.-J. 1992. Response of a stably stratified atmosphere to low-level heating — An application to the heat island problem. *J. App. Meteor.* **31**, 291–303.

Baik, J.-J. and Chun, H.-Y. 1996. Effects of nonlinearity on the atmospheric flow response to low-level heating in a uniform flow. *J. Atmos. Sci.* **53**, 1856–1869.

Booker, J. R. and Bretherton, F. R. 1967. The critical layer for internal gravity waves in a shear flow. *J. Fluid Mech.* **27**, 513–539.

Chun, H.-Y. 1991. *Role of a critical level in a shear flow with diabatic forcing.* PhD dissertation, North Carolina State University, 159 pp.

Chun, H.-Y. and Baik, J.-J. 1994. Weakly nonlinear response of a stably stratified atmosphere to diabatic forcing in a uniform flow. *J. Atmos. Sci.* **51**, 3109–3121.

Droegemeier, K. K. and Wilhelmson, R. B. 1985. Three-dimensional numerical modeling of convection produced by interacting thunderstorm outflow. Part I: Control simulation and low-level moisture variations. *J. Atmos. Sci.* **42**, 2381–2403.

Eliassen, A. and Palm, E. 1960. On the transfer of energy in stationary mountain waves. *Gephys. Publ.* **22**, 1–23.

Fovell, R. G. and Ogura, Y. 1989. Effect of vertical wind shear on numerical simulated muticell storm structure. *J. Atmos. Sci.* **46**, 3144–3176.

Fovell, R. G., Durran, D. and Holton, J. R. 1992. Numerical simulations of convectively generated stratospheric gravity waves. *J. Atmos. Sci.* **49**, 1427–1442.

Lin, Y.-L. 1987. Two-dimensional response of a stably stratified shear flow to diabatic heating. *J. Atmos Sci.* **44**, 1375–1393.

Lin, Y.-L. and Smith, R. B. 1986. Transient dynamics of airflow near a local heat source. *J. Atmos. Sci.* **43**, 40–49.

Lin, Y.-L. and Chun, H.-Y. 1991. Effects of diabatic cooling in a shear flow with a critical level. *J. Atmos. Sci.* **48**, 2476–2491.

Lindzen, R. S. 1981. Turbulence and stress owing to gravity wave and tidal breakdown. *J. Geophys. Res.* **86**, 9707–9714.

McFarlane, N. A. 1987. The effect of orgographically excited gravity wave drag on the general circulation of the lower stratosphere and troposphere. *J. Atmos. Sci.* **44**, 1775–1800.

Palmer, T. N., Shutts, G. J. and Swinbank, R. 1986. Alleviation of a systematic westerly bias in general circulation and numerical weather prediction models through anorographic gravity wave drag parametrization. *Quart. J. Roy. Meteor. Soc.* **112**, 1001–1039.

Pierrehumbert, R. T. 1986. An essay on the parametrization of orographical gravity wave drag. *Proc. Seminar/Workshop on Observation, theory and modeling of orographic effects.* 15–20 September ECMEWF, Shinfield Park, Reading, UK, **1**, 251–282.

Raymond, D. J. 1986. Prescribed heating of a stratified atmosphere as a model for moist convection. *J. Atmos. Sci.* **43**, 1101–1111.

Rotunno, R., Klemp, J. B. and Weisman, M. L. 1988. A theory for strong long-lived squall lines. *J. Atmos. Sci.* **45**, 463–485.

Smith, R. B. and Lin, Y.-L. 1982. The addition of heat to a stratified airstream with application to the dynamics of orographic rain. *Quat. J. Roy. Meteor. Soc.* **108**, 353–378.

Thorpe, A. J., Miller, M. and Moncrieff, M. W. 1980. Dynamical model of two-dimensional downdrafts. *Quat. J. Roy. Meteor. Soc.* **106**, 463–484.